Shear Strain Influence on Fiber Bragg Grating Measurement Systems

Mathias Stefan Müller, Thorbjörn C. Buck, Hala J. El-Khozondar, and Alexander Wilhelm Koch

***Abstract*—Fiber Bragg grating (FBG) sensors have become commercially available sensors for the measurement of temperature, strain, and many other quantities. One interesting application is the embedding of these sensors, during which shear strains can arise inside the sensor. As we have recently demonstrated by a full-tensor coupled-mode analysis, shear strains do influence the spectral response of fiber Bragg sensors, and thus have to be considered. In this paper, we use the theory behind this analysis to compute the direct influence of shear strains on the output of a FBG measurement system, and show cases where shear strain effects are relevant. Furthermore, we compare the sensitivity of different interrogation algorithms toward shear strain influences on the measurement system output. To model the experimentally relevant unpolarized light sources, we derive a model using the monochromatic waves of coupled-mode theory. We apply the unpolarized light to the FBG shear strain problem and show that for unpolarized light, shear strain has to be taken into account as well. We find absolute measurement errors in the range of 100 pm. For typical normal strain measurements, this would be of an order of 10% of relative error.**

***Index Terms*—Bragg scattering, measurement errors, optical fiber measurement applications, optical fiber polarization, strain measurement.**

I. Introduction

Fiber Bragg gratings (FBGs) have been considered for numerous sensing applications, including temperature, strain, and force, among others. One intriguing aspect is the possibility to extract two parameters from the sensor position by using a polarization-sensitive interrogation scheme. FBGs may be integrated into composite materials or concrete [1] due to their small dimensions. This possibility has gained much interest because reconstruction of the state of strain within such materials may improve applications such as condition monitoring.

A transversally loaded or embedded FBG will give an optical response corresponding to the strains that are distributed along the core of the fiber at the position of the sensor. This is due to the fact that light is only guided close to the fiber core, which is only around 10 μm in diameter, whereas the whole fiber measures approximately 100 μm. This approximation is called "center strain approximation" [2], and greatly simplifies the computation of the optical response of the FBG since transversal gradients in the strain field may be neglected. The loads applied to the fiber, either by transversal loading or embedding into a host material that is itself strained, as pictured in Fig. 1, will result in a position-dependent strain field within the fiber, represented by the strain tensor $\overline{\boldsymbol{e}}_{\mathrm{f}}(x,y,z)$. Since the dominant contribution to the change in the optical response of the FBG will result from the core of the fiber, we assume that $\overline{\boldsymbol{e}}_{\mathrm{c}}(z) = \overline{\boldsymbol{e}}_{\mathrm{f}}(0,0,z)$. The optical response of the grating upon this load is computed from coupled-mode theory (CMT). CMT is a widely employed tool, and has been applied to FBGs, as described in various articles, see, for example, [3] and [4].

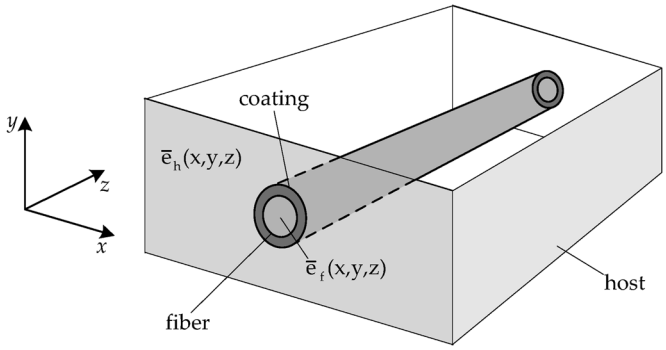

Fig. 1. Optical fiber with coating embedded into a host structure. The strains in the host $\overline{\boldsymbol{e}}_{\mathrm{h}}(x,y,z)$ will result in strains within the optical fiber $\overline{\boldsymbol{e}}_{\mathrm{f}}(x,y,z)$.

The influencing quantity $\overline{\boldsymbol{e}}_{\mathrm{c}}(z)$ is a tensor of second rank. It will, to first order, produce a dielectric perturbation in the fiber, which is also represented by a second-rank tensor, namely, the dielectric perturbation tensor $\Delta\overline{\boldsymbol{\varepsilon}}$ [5]. Each of the perturbation tensor's entries may be nonzero in an arbitrary load case. We recently demonstrated how the optical response of FBGs may be computed from the knowledge of this perturbation tensor by a full tensorial CMT [6], and derived a transfer matrix formalism for the problem [7]. We found that the strain tensor entries e_{xx}, e_{yy}, e_{zz}, and the shear strain e_{xy} show influences on the spectral response, and that the shear strain entries e_{xz} and e_{yz} possess virtually no influence, due to the very small longitudinal field components of the fundamental modes of the fiber.

The electromagnetic problem considers the four propagation modes of the fiber: two of orthogonal polarization p and s, propagating in positive z-direction, and two propagating in negative z-direction. The amplitudes of these four modes A_{p+}, A_{s+}, A_{p-}, and A_{s-} are coupled by the dielectric perturbations induced by the grating and the mechanical loads. In a polarization-maintaining fiber, the propagation constants of the mode

Manuscript received May 28, 2009; revised July 02, 2009. First published July 24, 2009; current version published October 07, 2009.

The authors are with the Institute for Measurement Systems and Sensor Technology, Technische Universität München, 80333 Munich, Germany (e-mail: m.s.mueller@tum.de; t.buck@tum.de; hkhozondar@iugaza.edu; a.w.koch@tum.de).

Digital Object Identifier 10.1109/JLT.2009.2028244

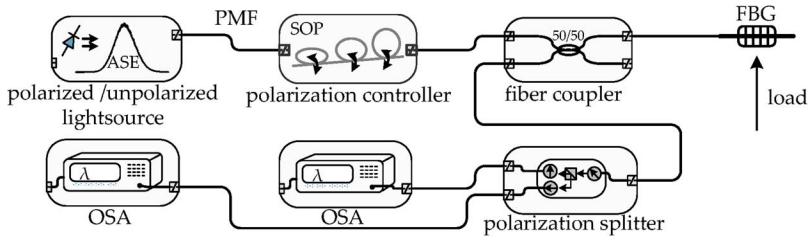

Fig. 2. Possible measurement setup for determining the spectral response of an FBG written in a polarization-maintaining fiber. The FBG is illuminated by a well-polarized source. Both axes of the polarization-maintaining fiber are illuminated equally. The reflected spectra are directed to a polarization splitter by a 3 dB fiber coupler. The polarization splitter splits the light in the fast and the slow polarization axes of the fiber. Both outputs are fed to two optical spectrum analyzers with low polarization dependency. For the whole setup, polarization-maintaining fibers are employed.

having orthogonal polarization $\beta_{p/s}$ differ by a value $\Delta\beta = 2\pi/L_B$, where L_B is called the beat length of the fiber. This difference in propagation constant will prevent the coupling of the polarization modes when the fiber is loaded mechanically, such as by twists or bends or other loads [8], [9]. However, this only works for moderate loads, and polarization coupling takes place when the fiber is loaded substantially.

When polarization-mode coupling is neglected, the two orthogonal polarizations may be used to measure two different parameters from the FBGs position [10], [11]. Then, only the three normal strains e_{xx}, e_{yy}, e_{zz}, and the temperature T have an influence on the optical response of the FBG. If all parameters are applied homogeneously along the length L of the grating, the Bragg reflection peaks of the two polarization axes will shift, without deforming their shape. The center wavelength of the two Bragg peaks is computed, and then, for example, the two normal strain entries e_{xx} and e_{yy} in the strain tensor may be reconstructed. The center wavelength is obtained by using algorithms such as maximum search, a centroid algorithm [12], or Gaussian fit [13].

This is only possible if the two other parameters, e_{xx} and T, are constant, which is not necessarily satisfied in each application. A solution has been suggested by Udd, giving an overview in [14]. The suggestion is to fabricate two Bragg gratings at the same position inside the fiber, with widely different wavelengths (1300 and 1500 nm). The fiber needs to be single mode in both wavelengths. If the material properties of the fiber (Pockel's coefficients and thermo-optic coefficient) are different at both wavelengths, it is possible to measure all four quantities with one sensor. In a recent work by Mawatari and Nelson [15] this suggestion is investigated. The authors note the necessity of being able to neglect polarization rotation within the fiber due to its polarization-holding capabilities. They state that the problem of reconstructing the four parameters would become much more complicated if such a polarization-mode coupling would occur.

The aim of our research is to study the influence of polarization-mode coupling within FBGs on the basis of the theory presented in [6]. We give a short summary on the theory and introduce the measurement setup we model with our simulations. We show how the parameter "shear strain," which has been widely ignored in the discussions on multiparameter strain sensing, has a significant influence on the response of such a sensor. For this purpose, we simulate the reflection spectrum of a mechanically loaded FBG sensor when shear strain is neglected and when shear strain effects are considered, and compare the results. Furthermore, we calculate the performance of three different peak fitting algorithms: maximum search, centroid, and Gaussian fit. To evaluate the outcome of an experiment incorporating shear strain and using an unpolarized light source, we introduce a model for unpolarized light using monochromatic waves. This becomes necessary since the underlying CMT model for computing the reflection of the FBG uses monochromatic waves. We demonstrate how shear strains also influence the response of an FBG measurement system when unpolarized light is used viz., a depolarizing element of some kind is employed. Parts of this paper have been already presented in [16].

II. Fundamentals and Theory

Several FBG interrogation schemes have been proposed to date. For the polarization-sensitive interrogation, a polarization-independent measurement is conducted, and the two Bragg peaks are separated by an algorithm [15] or the polarization spectra are recorded independently [17], [18]. We model the latter setup as it is in principle capable of providing more insights. A possible implementation of such a measurement system is illustrated in Fig. 2. We assume that either polarized light, with an angle of 45° with respect to the axes of the polarization-maintaining fiber is used to illuminate the Bragg grating, or, as a frequently used alternative, an unpolarized light source is employed. In both cases, the two reflected polarization spectra are split up by a polarization splitter or equivalent device and are directed to two polarization-independent optical spectrum analyzers or tunable Fabry Perot filters, etc.

A. Mechanical Test Case

In real-world applications, the strain tensor entries may vary independently of each other, giving a large range of parameters. In the transversal loading experiments [15], [17], [18], this range of parameters is reduced, since only two parameters, namely, the load angle ϕ and the load force F, are varied. This results in a strain tensor $\overline{\boldsymbol{e}}_{\mathrm{c}}$ that may be approximated by the form [6]

$$\overline{\boldsymbol{e}}_{\mathrm{c}}(\phi) = F\mathrm{R}(\phi)\begin{pmatrix} e_{xx} & 0 & 0 \\ 0 & -me_{xx} & 0 \\ 0 & 0 & 0 \end{pmatrix}\mathrm{R}(\phi)^T \qquad (1)$$

where $\mathrm{R}(\phi)$ is the rotation matrix around the z-axis. By rotating the fiber in the experiment, the shear strain e_{xy} is generated, which possesses a maximum value of approximately that of e_{xx}.

To further simplify the model, we restrict ourselves to the following load case. The only nonzero strain tensor entries are e_{xx}, $e_{yy} = -me_{xx}$, and e_{xy}. Entry e_{xx} is varied from 0 to 2000 μm/m, e_{yy} is scaled with $m = 0.2$, and e_{xy} is either zero, when neglecting shear strain effects, or possesses a value of $e_{xy} = 2000\ \mu\mathrm{m/m}$. The parameter m is determined by geometrical properties and material properties, such as Poisson's ratio and Young's modulus. For isotropic materials, an analytical treatment is given by Timoshenko and Goodier [19]. The chosen value is approximately that of Poisson's ratio of the fiber material. The exact value will, however, be different and could, for example, be predicted by a finite-element simulation. These parameters may very well be found in a real-world application. From the spectral information, the "Bragg-wavelength" has to be extracted. Therefore, several algorithms have been used. For a symmetrical Bragg peak, the algorithms—peak maximum, centroid, and Gaussian fit yield the same value. If the Bragg peak becomes unsymmetrical, the outputs of these algorithms will show differences. We apply the three algorithms to the two polarization-mode reflections separately.

B. Modeling of Polarized Light Source

Polarized light is characterized by the fact that the time dependence of the two polarization directions is fully correlated within the time of observation viz., the coherence length of both field components is long. The CMT model used in this paper uses monochromatic waves to compute the interaction of these waves at dielectric perturbations. Since monochromatic waves possess an infinite coherence length, both field components are fully correlated. Thus, the description of polarized light is easily possible. In a polarization-maintaining fiber, the direction of the electric fields of the two modes is fixed to the main axes of the fiber, and the polarization direction is thus fixed. However, there is a continuous retardation of both modes relative to one another, leading to the well-known beating effect in these fibers [20], [21]. This retardation may also be modeled using the monochromatic waves by introducing a relative z-dependent phase term $\phi(z)$. The normalized amplitudes of the monochromatic waves traveling in positive z-direction, and polarized parallel to the x axis $(p+)$ and parallel to the y axis $(s+)$ are thus described by

$$A_{p+} = \frac{1}{\sqrt{2}} \qquad A_{s+} = \frac{1}{\sqrt{2}} e^{i\phi(z)}. \tag{2}$$

The intensity of this field is equal to 1. For the ongoing computations, we assume the phase term $\phi(z)$ to be zero. We are aware that this represents a special case, but many effects may be well demonstrated under this assumption. Besides, this special case will frequently show up in FBG experiments.

C. Modeling of Unpolarized Light Source

The presented four wave model of FBGs is able to predict the interaction of monochromatic waves at a certain wavelength λ. By altering this wavelength and solving the coupled mode equations consecutively, we obtain the spectral response of the grating. Monochromatic waves, however, posses an infinite coherence length. The electric field of such a wave may be described by

$$E_x(z,t) = A_p \cos\left(\beta_p z - \omega t + \beta_x(t)\right) \tag{3}$$

$$E_y(z,t) = A_s \cos\left(\beta_s z - \omega t + \beta_y(t)\right). \tag{4}$$

This fact raises a problem when trying to incorporate effects such as depolarized or unpolarized light into the model. For unpolarized light, the correlation between the two polarization directions needs to be zero. This may not be fulfilled by purely monochromatic waves. For the description of unpolarized light, the Stokes parameters s_0, s_1, s_2, and s_3 may be used. An alternative description is given by using the coherence matrix [22]

$$\Phi_{ij} = \left\langle \varepsilon_i(t) \otimes \varepsilon_j^{\star}(t) \right\rangle \tag{5}$$

with $\varepsilon_1(t) = A_p(t)$, $\varepsilon_2(t) = A_p(t)\exp(i\delta(t))$, and $\delta(t) = \beta_s(t) - \beta_p(t)$. The brackets are indicating time averaging

$$\langle X(t) \rangle = \lim_{T\to\infty} \frac{1}{T} \int_0^T X(t)\mathrm{d}t. \tag{6}$$

A basis for the coherence matrix is given by

$$\boldsymbol{\sigma}_0 = \begin{pmatrix} 1 & 0 \\ 0 & 1 \end{pmatrix} \qquad \boldsymbol{\sigma}_1 = \begin{pmatrix} 1 & 0 \\ 0 & -1 \end{pmatrix} \tag{7}$$

$$\boldsymbol{\sigma}_2 = \begin{pmatrix} 0 & 1 \\ 1 & 0 \end{pmatrix} \qquad \boldsymbol{\sigma}_3 = \begin{pmatrix} 0 & -i \\ i & 0 \end{pmatrix}. \tag{8}$$

By these, the Stokes vector entries s_i may be computed using

$$s_i = \mathrm{tr}(\Phi \boldsymbol{\sigma}_i) \tag{9}$$

and from the Stokes vector, the degree of polarization is given by

$$P = \frac{\left(s_1^2 + s_2^2 + s_3^2\right)^{1/2}}{s_0}. \tag{10}$$

We intend to use the given description to assess the validity of a polarization model capable of describing unpolarized light using the monochromatic waves of the FBG model. The idea is to construct a signal consisting of a series of monochromatic waves with different states of polarization. Such an approach has been demonstrated by Jizhong [23]. By choosing the polarization of each wave in an appropriate way, the constructed signal will show the required low degree of polarization. It is then possible to feed the individual signals, each with a different polarization to the FBG model, and sum up the resulting output intensities for each polarization. This will give the response of the FBG for unpolarized incident light.

The trace of the coherence matrix represents the intensity of the light $I = \mathrm{tr}(\Phi)$, which is kept constant. Hence, the monochromatic wave—unpolarized light model—is constructed using the $l = m \cdot n$ individual waves

$$A_{p,l} = \cos(\phi_{1,n}) \tag{11}$$

$$A_{s,l} = \sin(\phi_{1,n}) e^{i\phi_{2,m}} \tag{12}$$

with $\phi_{1,1\ldots N}, \phi_{2,1\ldots N} = \{0, 2\pi/N, \ldots, 2\pi(1-1/N)\}$. The variables ϕ_1 and ϕ_2 represent the 2 DOF—polarization direction and relative phase of the two fields. The positive integer N

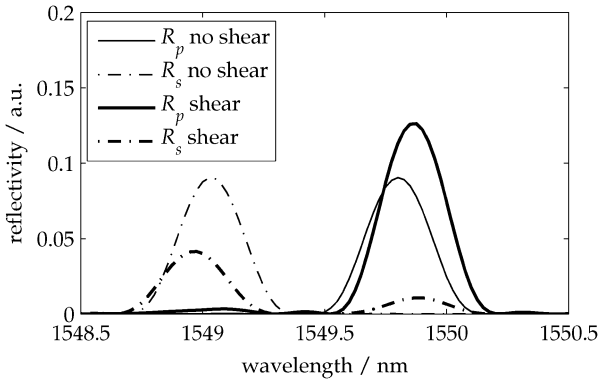

Fig. 3. Result of the simulation using a normal strain $e_{xx} = 2000\,\mu\mathrm{m/m}$ and $e_{yy} = -m e_{xx}$, $m = 0.2$. The shear strain is neglected in the thin-lined result and set to 2000 $\mu\mathrm{m/m}$ for the simulation with shear strain. The results without shear strain show the expected shift of the spectral response, without changing the shape of the spectrum. With shear strain, the polarization modes couple and the reflection spectra are changed in shape.

is the number of polarization directions and phase differences, respectively.

Choosing N to be 50, the computed coherence matrix ϕ of the model becomes diagonal, representing fully unpolarized light [24]. However, this may also be an artefact of the way we constructed the series of monochromatic waves. To have an independent measure of the quality of approximation of unpolarized light, we choose N random values of ϕ_1 and ϕ_2 between 0 and 2π, and compute the degree of polarization P for each random set. The mean degree of polarization $\bar{P}$ over several sets is evaluated. We expect $\bar{P}$ to decrease for higher N. This is confirmed by our results. For a random set of $N = 50$, the mean degree of polarization is approximately 8%.

For further modeling of unpolarized light, we chose $N = 10$, and thus run the FBG simulation procedure with 100 different incident polarizations for each wavelength point. The computed degree of polarization of this wave is zero. The l reflected amplitudes $A_{p-,l}$ and $A_{s-,l}$ each contribute to the detected reflection intensities $I_{p,r}$ and $I_{s,r}$ at a certain wavelength, giving

$$I_{p,r} = \frac{1}{l}\sum_{j=1}^{l} |A_{p-,l}|^2 \qquad I_{s,r} = \frac{1}{l}\sum_{j=1}^{l} |A_{s-,l}|^2. \qquad (13)$$

III. Results and Discussion

A. Polarized Light

The first load case is computed to illustrate in detail the influence of shear strain on the reflection spectra. A normal strain $e_{xx} = 2000\ \mu\mathrm{m/m}$ and a shear strain $e_{xy} = 2000\ \mu\mathrm{m/m}$ is used. Fig. 3 shows the computed result both neglecting shear strain and taking into account shear strain.

As may be seen from the results that neglecting shear strain, the spectral shapes of both Bragg peaks are symmetric. They are shifted by some amount according to the load, but do not change their spectral characteristic. The reflection spectra considering shear strain do change their characteristics. The left peak corresponding to the s polarization couples intensity into the right peak corresponding to the p polarization. This would by itself not change the output of the peak-finding algorithms. But what

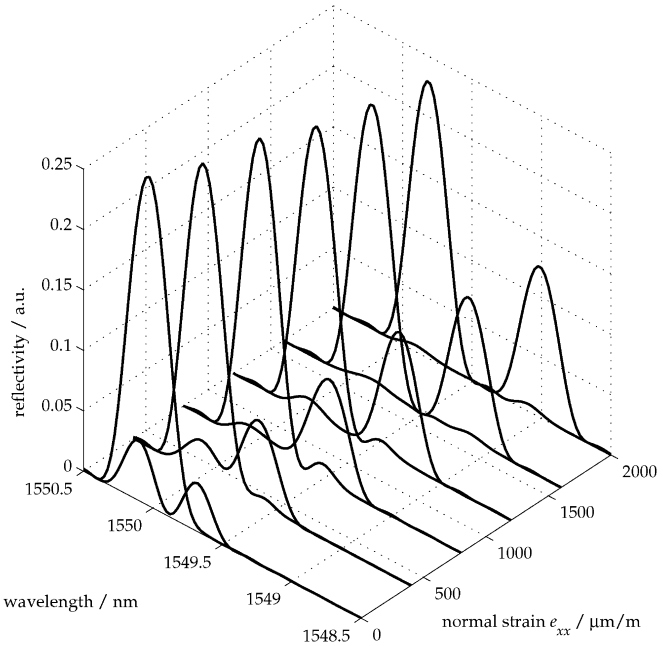

Fig. 4. Six simulations with increasing normal strain and a fixed shear strain of $e_{xy} = 1000\ \mu\mathrm{m/m}$. For low normal strains, the reflection peaks are only separated by the birefringence of the fiber and polarization-mode coupling is high, leading to a strong second peak in the s-mode reflection spectrum. For higher normal strain loads, peak separation is increased and polarization-mode coupling is reduced.

may also be observed is that the shear strain changes the spectral position of the peaks, something that would yield a different result. Apart from this, a second-order effect may be observed when taking a look at the s-mode's intensity at the position of the p-mode's reflection peak. Here, due to polarization-mode coupling, the backward propagating p-mode couples onto the backward propagating s-mode. This leads to a second peak in the s-mode spectrum, something that has been observed by Ye *et al.* [18] in their lateral loading experiment, attributing it to structural changes in the polarization-maintaining fiber.

To precisely study the effect, the reflection spectra of the Bragg grating are computed for increasing load $e_{xx} = \{0, 400, 800, 1200, 1600, 2000\}\ \mu\mathrm{m/m}$ and e_{yy} accordingly. e_{xy} is fixed to 2000 $\mu\mathrm{m/m}$. For low e_{xx}, the two peaks are separated by the fiber's birefringence only, and the polarization modes are strongly coupled. This results in a s-mode reflection peak, which nearly possesses two equally strong maxims. For increasing normal strain, the separation of the polarization modes' reflection peaks increases, and the propagation constant difference increases, leading to lower polarization-mode coupling. Hence, the second maxima in the s-mode reflection decreases.

Calculating the response of the interrogation algorithms, we use the loads described before. We compute the output of the measurement setup for two different kinds of fibers. Since polarization-mode coupling will increase with increasing beat length L_B, we use the beat length values of 7.7 and 3.0 mm. These fibers are commercially available and represent the lower end of available beat lengths. Thus, polarization-mode coupling is generally low in the selected fibers and effects may be expected to increase with higher beat lengths.

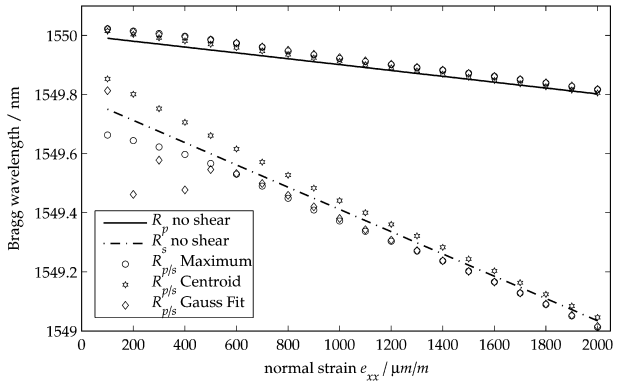

Fig. 5. Computation of the Bragg wavelength of the s- and p-modes by three algorithms —maximum search, Gaussian fit, and centroid. For comparison, the Bragg wavelength neglecting shear strain influences is computed. For symmetrical reflection peaks, all three algorithms yield the same result; therefore, the result without shear is independent of the algorithm used. This figure show the simulation results for a fiber with a lower birefringence and a beat length of $L_B = 7.7$ mm.

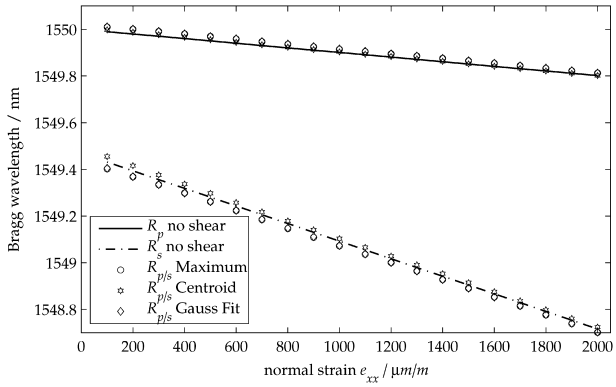

Fig. 6. Computation of the Bragg wavelength of the s- and p-modes by three algorithms—maximum search, Gaussian fit, and centroid. For comparison, the Bragg wavelength neglecting shear strain influences is computed. For symmetrical reflection peaks, all three algorithms yield the same result; therefore, the result without shear is independent of the algorithm used. The figure corresponds to a fiber with a birefringence corresponding to a beat length of $L_B = 3.0$ mm.

Fig. 5 shows the results for $L_B = 7.7$ mm. The lower values correspond to the Bragg wavelength of the s-mode reflection spectrum, and those at higher wavelengths correspond to the p-mode reflection. The p-mode's spectral response is less deformed in shape than the s-mode. This is simply determined by the positive sign of the shear strain, using a negative value, and the p-mode would be deformed in a comparable way. It is observed that the values for the p-mode Bragg wavelength are all situated at higher wavelengths than without shear strain.

This is something that may be explained by the spectral shift to higher values, shown in Fig. 3. Yet the s-modes' results show positive as well as negative differences. This may be explained as follows. The maximum of the s-modes' Bragg peak with shear strain is at lower wavelengths than without shear strain. This also yields lower values for the maximum algorithm. The Gaussian fit applies to the strong left peak of the s-mode in Fig. 3, but the centroid algorithm integrates the whole spectrum and weights it with the spectral position. This gives the right second peak in the s-modes reflection spectrum a special influence on the position of the Bragg wavelength. For low normal strains, the polarization-mode coupling is the strongest, leading to a strong second peak in the s-modes reflection spectrum. The Gaussian fit algorithm will either fit to one or the other, yielding strong deviations.

If the beat length is increased viz., the birefringence of the fiber is higher, the polarization-mode coupling is reduced, and the effects are smaller. This may be observed by comparing Fig. 5 and Fig. 6. Due to the higher birefringence, the reflection peaks of the polarization modes are separated stronger initially, leading to a different scaling of the plots.

The effect of polarization cross coupling results in a measurement error in the determination of the actual Bragg wavelength, since the spectral response is deformed. This interferes with the concept of multiparameter strain sensing, as suggested by Udd [14]. The shear strain component e_{xy} has to be considered as an individual parameter, yielding a total of five parameters. These are e_{xx}, e_{yy}, e_{xy}, e_{zz}, and T. The four values extracted from the four Bragg peaks, as suggested by Udd, thus yield a singular problem.

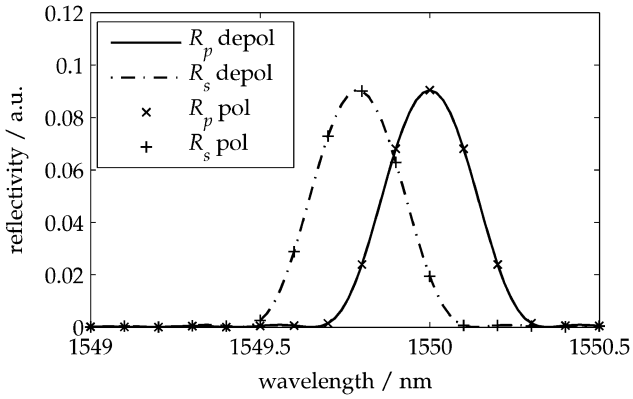

Fig. 7. Testing of the model of unpolarized light by simulating a FBG response without shear effects. The polarized and unpolarized light sources should show the same reflection spectra, as confirmed by the plot.

B. Unpolarized Light

Before demonstrating the results of shear-strain-loaded FBGs when illuminated with unpolarized light, we need to confirm the applicability of our model for unpolarized light. We, therefore, compute the response of an FBG in a polarization-maintaining fiber in the absence of shear strain. For this case, the result for polarized light with $A_{p+} = 1/\sqrt{2}$ and $A_{s+} = 1/\sqrt{2}$, and fully unpolarized light need to be the same. Fig. 7 shows the results of both computations. As is to be expected, both light sources are yielding the same results.

As a next step, we are interested in whether by using an unpolarized light source, the effects of shear strain on the FBG reflection response may be changed or even canceled out. Therefore, we use the mechanical model of the preceding section with $e_{xx} = 2000\ \mu\mathrm{m/m}$ and $e_{xy} = 2000\ \mu\mathrm{m/m}$. The result of this computation is given in Fig. 8. When comparing the lines corresponding to a simulation neglecting shear strain with those taking into account shear strain and using an unpolarized light source, it is notable that a small shift of the main peaks in wavelength occurs. The two main peaks stem from the conventional Bragg reflection at the Bragg wavelength shifted by the normal strains e_{xx} and e_{yy}, plus an additional effect from the

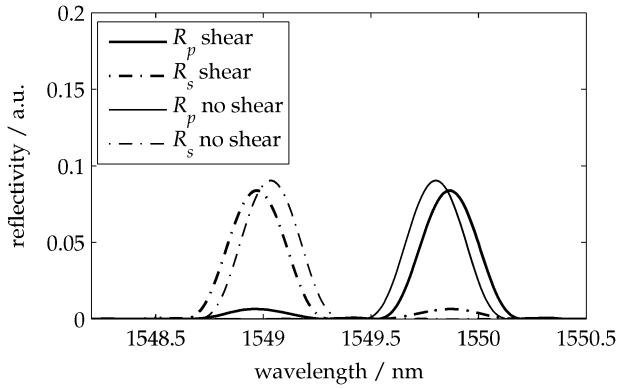

Fig. 8. Shear-strain-loaded FBG in polarization-maintaining fiber illuminated with unpolarized light. The loading strains are $e_{xx} = 2000\ \mu\mathrm{m/m}$, $e_{yy} = -me_{xx}$, $m = 0.2$, and $e_{xy} = 2000\ \mu\mathrm{m/m}$. A shear-strain-assisted polarization-mode coupling may be observed at the position of the main peak in the intensity distribution of the orthogonal polarization direction.

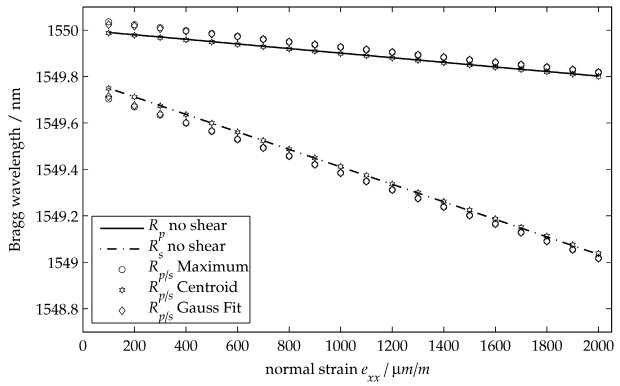

Fig. 9. Response of the depolarized FBG measurement system using three different peak searching algorithms, upon shear strain. The results show a clear deviation from the ideal line, neglecting shear strain influences.

shear strain. Two secondary peaks at the position of these main peaks may be observed, yet in the orthogonal field component. These peaks are again a result of shear-strain-assisted polarization-mode coupling within the grating, as we describe in [6]. This implies that the shear strain e_{xy} will change the spectral response, and thus have an influence on the output of an FBG measurement system again.

To gain an insight into the influence on a depolarized measurement system, we compare the results of the three frequently employed peak searching algorithms of Section III-A. We model an FBG in a polarization-maintaining fiber with a beat length of $L_B = 7.7$ mm and a constant shear strain of 2000 $\mu\mathrm{m/m}$. The normal strains are increased from 0 to 2000 $\mu\mathrm{m/m}$, and the algorithms are applied to the two polarization directions' reflection spectra.

The results shown in Fig. 9 show a clear deviation from the ideal line, neglecting shear strain for the Gaussian fit and the maximum search algorithm. This may be understood from the results in Fig. 8. The shear-strain-loaded response shows a shift in the main Bragg peaks' wavelength. These two algorithms are more sensitive to the main peak. The centroid algorithm, however, takes into account the weight of every contribution of the spectrum equally. This means that the shift of the main Bragg peaks position due to shear strain gets somewhat compensated for by the secondary peaks, also caused by shear-strain-assisted polarization-mode coupling. This implies that shear strain effects play a role even in depolarized FBG measurement systems.

IV. Conclusion and Outlook

In this paper, we applied full tensor CMT to compute the optical response of a mechanically loaded FBG in a polarization-maintaining fiber in the presence of strong shear strains. We constructed a representative load case that may occur in a fiber sensing application. For several load scenarios, we calculated the output spectrum for the two polarization modes. We used these data to test three algorithms to determine the Bragg wavelength-maximum search, centroid, and Gaussian fit. We demonstrated how the algorithms perform for two different types of polarization-maintaining fibers having different beat lengths. As expected, we found a reduced influence of shear strain if fibers with high birefringence are employed. For a case of $L_B = 7.7$ mm, the deviations of the Bragg peak caused by shear strain were found to exceed 100 pm.

Thus, a load case that comprises identical normal strains, but different shear strains may lead to strongly differing results. Comparing the values to a temperature measurement, the 100 pm would correspond to approximately 10 °C or 100 $\mu\mathrm{m/m}$. As a result, shear strain has to be considered as a parameter influencing the output of an FBG measurement system. We also demonstrated how a model for unpolarized light may be established using monochromatic waves used for the CMT. We applied this model to calculate the response of shear-strain-loaded FBGs for a measurement system using a depolarization unit. The results demonstrate that depolarizing the light source does not cancel the shear strain effects. These have to be taken into account in this case also. An exception was made by the centroid algorithm that seemed to cancel the shear strain effects for the studied case. Yet there may be other cases for which the centroid algorithm might not provide such a kind of compensation.

This has implications for the method of reconstructing the three normal strains and temperature, as proposed by Udd [14]. Since five parameters are actually influencing the spectral response significantly, the four parameters derived from the proposed experiment will not suffice to reconstruct the state of strain.

However, it may be observed that the relative power of the polarization reflection peaks is depending on the applied shear strain. It may therefore be possible to use this dependency to reconstruct a fifth parameter, possibly directly the shear strain component e_{xy}, from the relative intensities of the two Bragg peaks. This should then allow to overcome the singularity of the problem and provide a method that allows the reconstruction of the full strain tensor by a single FBG sensor.

References

[1] J. Calero, S.-P. Wu, C. Pope, S. Chuang, and J. Murtha, "Theory and experiments on birefringent optical fibers embedded in concrete structures," *J. Lightw. Technol.*, vol. 12, no. 6, pp. 1081–1091, Jun. 1994.

[2] M. Prabhugoud and K. Peters, "Finite element model for embedded fiber Bragg grating sensor," *Smart Mater. Struct.*, vol. 15, pp. 550–562, 2006.

[3] M. McCall, "On the application of coupled mode theory for modeling fiber Bragg gratings," *J. Lightw. Technol.*, vol. 18, no. 2, pp. 236–242, Feb. 2000.
[4] T. Erdogan, "Fiber grating spectra," *J. Lightw. Technol.*, vol. 15, no. 8, p. 1277, Aug. 1997.
[5] T. Narasimhamutry, *Photoelastic and Electro-Optic Properties of Crystals*. New York: Plenum, 1981.
[6] M. S. Müller, L. Hoffmann, A. Sandmair, and A. W. Koch, "Full strain tensor treatment of fiber Bragg grating sensors," *IEEE J. Quantum Electron.*, vol. 45, no. 5, pp. 547–553, May 2009.
[7] M. S. Müller, H. El-Khozondar, A. Bernardini, and A. W. Koch, "Transfer matrix approach to four mode coupling in fiber Bragg gratings," *IEEE J. Quantum Electron.*, vol. 45, no. 9, pp. 1142–1148, Sep. 2009, accepted for publication.
[8] R. Ulrich and A. Simon, "Polarization optics of twisted single-mode fibers," *Appl. Opt.*, vol. 18, pp. 2241–2251, 1979.
[9] S. Rashleigh, W. Burns, R. Moeller, and R. Ulrich, "Polarization holding in birefringent single-mode fibers," *Opt. Lett.*, vol. 7, pp. 40–42, 1982.
[10] R. Gafsi and M. El-Sherif, "Analysis of induced-birefringence effects on fiber Bragg gratings," *Opt. Fiber Technol.*, vol. 6, pp. 299–323, 2000.
[11] C. Lawrence, D. Nelson, E. Udd, and T. Bennett, "A fiber optic sensor for transverse strain measurement," *Exp. Mech.*, vol. 39, no. 3, pp. 202–209, 1999.
[12] A. Ezbiri, S. Kanellopoulos, and V. Handerek, "High resolution instrumentation system for fibre-Bragg grating aerospace sensors," *Opt. Commun.*, vol. 150, pp. 43–48, 1998.
[13] H. W. Lee and M. Song, "FBG interrogation with a scanning Fabry–Perot filter and Gaussian line-fitting algorithm," in *Proc. 18th Annu. Meeting IEEE Lasers Electro-Opt. Soc.*, 2005, pp. 963–964.
[14] E. Udd, "Review of multi-parameter fiber grating sensors," in *Proc. Fiber Opt. Sens. Appl. V, Proc. SPIE*, 2007, pp. 677002.1–677002.10.
[15] T. Mawatari and D. Nelson, "A multi-parameter Bragg grating fiber optic sensor and triaxial strain measurement," *Smart Mater. Struct.*, vol. 17, pp. 035033-1–035033-19, 2008.
[16] M. S. Müller, T. C. Buck, H. J. El-Khozondar, and A. W. Koch, "Measurement errors from internal shear strain within fiber-Bragg-grating sensors," in *Proc. SPIE Eur.-Opt. Metrol.*, 2009, pp. 739007-1–739007-8, to be published.
[17] E. Chehura, C. Ye, S. Staines, S. James, and R. Tatam, "Characterization of the response of fibre Bragg gratings fabricated in stress and geometrically induced high birefringent fibres to temperature and transverse load," *Smart Mater. Struct.*, vol. 13, pp. 888–895, 2004.
[18] C.-C. Ye, S. E. Staines, S. W. James, and R. P. Tatam, "A polarization-maintaining fibre Bragg grating interrogation system for multi axis strain sensing," *Meas. Sci. Technol.*, vol. 13, pp. 1446–1449, 2002.
[19] S. Timoshenko and J. Goodier, *Theory of Elasticity*, ser. Engineering Societies Monographs. New York: McGraw-Hill, 1951.
[20] J. Noda, "Polarization-maintaining fibers and their applications," *J. Lightw. Technol.*, vol. LT-4, no. 8, pp. 1071–1089, Aug. 1986.
[21] I. Kaminow, "Polarization in optical fibers," *IEEE J. Quantum Electron.*, vol. QE-17, no. 1, pp. 15–22, Jan. 1981.
[22] J. Gil, "Polarimetric characterization of light and media," *Eur. Phys. J. Appl. Phys.*, vol. 40, pp. 1–47, 2007.
[23] W. Jizhong, "A matrix method for describing unpolarized light and its applications," *Acta Mech. Sin.*, vol. 2, pp. 362–372, 1986.
[24] M. Born and E. Wolf, *Principles of Optics*. Cambridge, U.K.: Cambridge Univ. Press, 2005.
[25] J. Zhao, X. Zhang, Y. Huang, and X. Ren, "Experimental analysis of birefringence effects on fiber Bragg gratings induced by lateral compression," *Opt. Commun.*, vol. 229, pp. 203–207, 2003.

Mathias Stefan Müller was born in Germany in 1980. He received the Dipl.-Ing. degree in electrical engineering and information technology from the Technische Universität München, Munich, Germany.

Since 2006, he has been with the Institute for Measurement Systems and Sensor Technology, Technische Universität München, where he started his research on optomechanical interactions in fiber Bragg grating sensors. He completed the Diploma thesis in the field of fiber optic sensors in 2006.

Thorbjörn C. Buck was born in Germany in 1982. He received the Dipl.-Phys. degree in physics from the Technische Universität München, Munich, Germany, in 2008.

Since 2008, he has been with the Institute for Measurement Systems and Sensor Technology, Technische Universität München, where he started his research on interrogators for fiber Bragg grating sensors. He completed the Diploma thesis in the field of terahertz imaging.

Hala J. El-Khozondar received the B.Sc. in physics degree from BirZeit University, BirZeit, Palestinian, in 1987, and the Ph.D. degree in physics from New Mexico State University, Las Cruces, in 1999.

In 1987, she joined the Physics Faculty, BirZeit University. In 1999, she received the Postdoctoral Award from Max Planck Institute, Heidelberg, Germany. During 2000, she was an Assistant Professor in electrical and computer engineering at Islamic University of Gaza. She is currently with the Institute for Measurement Systems and Sensor Technology, Technische Universität München, Munich, Germany. Her research interests include studying optical fiber sensors, magneto-optical isolators, optical filter, mobile-trusted-modules devices, electro-optical waveguides, and numerical simulation of microstructural evolution of polycrystalline materials.

Dr. El-Khozondar was a recipient of international awards and recognitions, including the Fulbright Scholarship, German Academic Exchange Service short study visit, the Alexander von Humboldt-Stiftung Scholarship, and the Erasmus Mundus.

Alexander Wilhelm Koch received the diploma in electrical engineering and information technology in 1983 and the Doctor of Engineering degree from the Universität der Bundeswehr, Munich, Germany in 1988. From 1988 to 1992, he was a Postdoctoral Researcher with the Max-Planck-Society. In 1992, he received the habilitation degree in electrophysics.

From 1988 to 1992, he was a Postdoctoral Researcher at Max Planck Society. From 1992 to 1998, he was a Professor of measurement science at the Universität Saarbrücken. Since 1998, he has been the Chair and the Director of the Institute for Measurement Systems and Sensor Technology, Technische Universität München, Munich, Germany. His current research interests include multisensory systems, optical measurement technology, laser- and video-based perceptions, environmental monitoring, optical fiber sensors, speckle-holographic measurement techniques, and image processing.